The Atrial Natriuretic Peptide and Guanylyl Cyclase-A System Modulates Pancreatic β-Cell Function

Ana B. Ropero, Sergi Soriano, Eva Tudurí, Laura Marroquí, Noelia Téllez, Birgit Gassner, Pablo Juan-Picó, Eduard Montanya, Ivan Quesada, Michaela Kuhn, and Angel Nadal

Centro de Investigación Biomédica en Red de Diabetes y Enfermedades Metabólicas Asociadas and Instituto de Bioingeniería (A.B.R., S.S., E.T., L.M., P.J.-P., I.Q., A.N.), Universidad Miguel Hernández de Elche, 03202 Elche, Spain; Centro de Investigación Biomédica en Red de Diabetes y Enfermedades Metabólicas Asociadas (N.T., E.M.), Hospital Universitari Bellvitge and Laboratory of Diabetes and Experimental Endocrinology, Department of Clinical Sciences, Institut d'Investigació Biomèdica de Bellvitge-University of Barcelona, L'Hospitalet de Llobregat, 08907 Barcelona, Spain; and Institute of Physiology (B.G., M.K.), University of Würzburg, Würzburg, Germany

Atrial natriuretic peptide (ANP) and its guanylyl cyclase-A (GC-A) receptor are being involved in metabolism, although their role in the endocrine pancreas is still greatly unknown. The aim of this work is to study a possible role for the ANP/GC-A system in modulating pancreatic β-cell function. The results presented here show a direct effect of the GC-A receptor in regulating glucose-stimulated insulin secretion (GSIS) and β-cell mass. GC-A activation by its natural ligand, ANP, rapidly blocked ATP-dependent potassium (K_{ATP}) channel activity, increased glucose-elicited Ca^{2+} signals, and enhanced GSIS in islets of Langerhans. The effect in GSIS was inhibited in islets from GC-A knockout (KO) mice. Pancreatic islets from GC-A KO mice responded to increasing glucose concentrations with enhanced insulin secretion compared with wild type (WT). Remarkably, islets from GC-A KO mice were smaller, presented lower β-cell mass and decreased insulin content. However, glucose-induced Ca^{2+} response was more vigorous in GC-A KO islets, and basal K_{ATP} channel activity in GC-A KO β-cells was greatly diminished compared with WT. When protein levels of the two K_{ATP} channel constitutive subunits sulfonylurea receptor 1 and Inward rectifier potassium channel 6.2 were measured, both were diminished in GC-A KO islets. These alterations on β-cell function were not associated with disruption of glucose tolerance or insulin sensitivity *in vivo*. Glucose and insulin tolerance tests were similar in WT and GC-A KO mice. Our data suggest that the ANP/GC-A system may have a modulating effect on β-cell function. **(*Endocrinology* 151: 3665–3674, 2010)**

Atrial natriuretic peptide (ANP) is a component of the natriuretic peptide family, which also includes brain natriuretic peptide (BNP), and C-type natriuretic peptide. The main receptor for ANP is guanylyl cyclase-A (GC-A/Npr-A). This receptor is a member of the family of GCs comprising GC-A to GC-G (1, 2). ANP and GC-A are involved in maintaining blood pressure and cardiac growth. In fact, ANP knockout (KO) and GC-A KO mice share hypertension and cardiac hypertrophy (2). Recent studies suggest a role for natriuretic peptides and their receptors in modulating metabolism through increasing lipolysis (3–6). Elevated plasma levels of ANP are found during acute hyperglycemia in type 1 diabetes mellitus (7), and ventricular ANP gene expression is increased in streptozotocin-induced diabetic rats (8).

The islet of Langerhans is the main tissue involved in maintaining blood glucose homeostasis, and its dysfunction is an essential factor in the development of type 1 and

ISSN Print 0013-7227 ISSN Online 1945-7170
Printed in U.S.A.

doi: 10.1210/en.2010-0119 Received January 28, 2010. Accepted May 18, 2010.
First Published Online June 16, 2010

Abbreviations: ANP, Atrial natriuretic peptide; AUC, area under the curve; BNP, brain natriuretic peptide; GSIS, glucose-stimulated insulin secretion; GC, guanylyl cyclase; GSIS, glucose-stimulated insulin secretion; IPGTT, intraperitoneal glucose tolerance test; ITT, insulin tolerance test; K_{ATP}, ATP-dependent potassium; Kir6.2, inward rectifier potassium channel 6.2; KO, knockout; NADH, reduced nicotinamide adenine dinucleotide; NP_o, mean open probability; Sur1, sulfonylurea receptor 1; WT, wild type.

type 2 diabetes mellitus (9, 10). Insulin secretion in pancreatic β-cells is driven by the ATP-dependent potassium (K_{ATP}) channels and calcium entry (11).

It has been shown that GC-A is present in pancreatic β-cells (12, 13). Interestingly, You and Laychock (13) have demonstrated that ANP, likely through activation of GC-A, regulates pancreatic β-cell growth. A possible insulinotropic action for ANP/GC-A is still a matter of controversy. It was demonstrated that ANP elicits an increase in circulating insulin in humans (14) and stimulates insulin secretion in rats (15), whereas in other studies, ANP produced no significant insulinotropic action or even inhibited glucose-stimulated insulin secretion (GSIS) (13, 16, 17). Cyclic GMP, the second messenger produced by the activation of GC-A by ANP, blocks K_{ATP} channels and enhances glucose-induced calcium signaling in mouse β-cells (18). Moreover, GC-A is involved in the insulinotropic effect of 17β-estradiol in mouse β-cells through modulation of K_{ATP} channels (12).

The aim of this work is to study a possible role for the ANP/GC-A system in modulating pancreatic β-cell function.

Materials and Methods

Materials

Fura 2-acetoxymethyl ester was obtained from Molecular Probes (Invitrogen, Barcelona, Spain) and human insulin from Lilly (Humulina Regular, Madrid, Spain). All other chemicals were obtained from Sigma (Madrid, Spain).

Animals

Female mice with global deletion of GC-A (GC-A KO) and corresponding wild-type (WT) mice were generated by the group of D. L. Garbers (University of Texas Southwestern Medical Center, Dallas, TX) (19). Other mice used in this work are C57 female and OF-1 male and female. Mice were 3–4 months old, unless otherwise stated. All animals were kept under standard housing conditions. A committee on internal animal care and use reviewed and approved the method used.

Islet and islet cells isolation

Pancreatic islets of Langerhans were isolated by collagenase (Sigma) digestion as previously described (20). Islets were dispersed into single cells with trypsin. Cells were then centrifuged and resuspended in RPMI 1640 without phenol-red (Invitrogen) and with 10% charcoal dextran-treated fetal bovine serum (HyClone, Logan, UT), 2 mM L-glutamine, 200 U/ml penicillin, and 0.2 mg/ml streptomycin. Cells were then plated in covers and used within 24 h of culture.

Patch-clamp recordings

K_{ATP} channel activity was recorded using standard patch-clamp recording procedures from isolated islet cells. Currents were recorded using an Axopatch 200B patch-clamp amplifier (Axon Instruments Co., Union City, CA). Patch pipettes were pulled from borosilicate capillaries (Sutter Instruments Co., Novato, CA) using a flaming/brown micropipette puller P-97 (Sutter Instruments Co.) with resistance between 3–5 MΩ when filled with the pipettes solutions as specified below. Bath solution contained (in mM): 5 KCl, 135 NaCl, 2.5 $CaCl_2$, 10 HEPES, and 1.1 $MgCl_2$ (pH 7.4) and supplemented with glucose as indicated. The pipette solution contained (in mM): 140 KCl, 1 $MgCl_2$, 10 HEPES, and 1 EGTA (pH 7.2). The pipette potential was held at 0 mV throughout recording. K_{ATP} channel activity was quantified by digitizing 60-sec sections of the current record, filtered at 1 kHz, sampled at 10 kHz by a Digidata 1322A (Axon Instruments Co.), and calculating the mean open probability (NP_o) of the channel during the sweep. Channel activity was defined as the product of N, the number of functional channels, and P_o, the open-state probability. P_o was determined by dividing the total time channels spent in the open state by the total sample time. Data sampling was started 1 min before (control) and 5 min after application of test substances. Experiments were carried out at room temperature (20–24 C).

Insulin secretion measurement

Pancreatic islets of Langerhans were cultured in the same medium as islet cells described above. After 24 h in culture, islets were incubated at 37 C in groups of five islets in a buffer solution containing 120 mM NaCl, 25 mM $NaHCO_3$, 5 mM KCl, 2.5 mM $CaCl_2$, 1 mM $MgCl_2$, and 3 mM D-glucose (final pH 7.35). After 2 h, the solution was replaced by fresh solution containing the different stimuli, and the islets were incubated for an additional hour at 37 C. Afterwards, the medium was collected, and insulin was measured in duplicate samples by RIA using a Coat-a-Count kit (Siemens, Los Angeles, CA).

Insulin content measurement

Freshly isolated islets were hand picked in batches of 10 and lysed overnight in an ethanol/HCl buffer at 4 C. Islets from the insulin secretion experiments were subjected to the same protocol. After the overnight incubation, the buffer was removed, and insulin was determined by RIA. Protein content was determined using the Bradford dye method.

Recording $[Ca^{2+}]_i$

Freshly isolated islets of Langerhans were loaded with 5 μM Fura 2-acetoxymethyl ester for at least 1 h at room temperature. Calcium recordings in the whole islet of Langerhans were obtained by imaging intracellular calcium under an inverted epifluorescence microscope (Axiovert 200; Zeiss, Jena, Germany). Images were acquired every 2 sec with an extended Hamamatsu Digital Camera C4742-95 (Hamamatsu Photonics, Barcelona, Spain) using a dual filter wheel (Sutter Instrument Co.) equipped with 340 and 380 nm, 10-nm bandpass filters (Omega Optics, Madrid, Spain). Data were acquired using Aquacosmos software from Hamamatsu (Hamamatsu Photonics). Fluorescence changes are expressed as the ratio of fluorescence at 340 and 380 nm (F340/F380). Results were plotted and analyzed using commercially available software (Sigmaplot; Jandel Scientific, Corte Madera, CA).

Islet size

Transmission images from isolated whole islets were taken using a confocal Zeiss Pascal 5 microscope and a Zeiss ×40 objective

(numerical aperture, 1.3). Islets were focused in the plane with the maximum area, and images were taken. Afterwards, the area of those planes was quantified using LSM Zeiss software (Zeiss) as μm^2 and used as the "islet size." At least 400 islets from three different mice were measured per condition.

β-Cell mass

Mice were anesthetized with a combination of ketamine (70 mg/kg), diazepam (5.6 mg/kg), and atropine (0.5 mg/kg). A midlaparotomy was performed, the pancreas was exposed, the animal was killed, and the pancreas was immediately dissected from surrounding tissues, cleared of fat and lymph nodes, blotted, weighed, and fixed in 4% paraformaldehyde fixative and processed for paraffin embedding. The weight of the pancreas was determined on a Mettler balance type A240 reading to 0.01 mg (Mettler Instruments Corp., Hightstown, NJ). β-Cell mass was measured by point-counting morphometry on immunoperoxidase-stained sections for insulin [rabbit antihuman insulin antibody (1:50); Santa Cruz Biotechnology, Inc., Santa Cruz, CA], using a 48-point grid to obtain the number of intercepts over β-cells (21, 22). β-Cell mass was obtained by multiplying the weight of the graft by the relative β-cell volume.

In vivo experiments

All the *in vivo* experiments were performed in between 0800 and 1000 h. Blood glucose was obtained from the tail vein using an Accu-check portable glucometer (Roche Diagnostic GmbH, Mannheim, Germany). For determination of fasting blood glucose levels and the ip glucose tolerance test (IPGTT), mice were separated the previous evening and fasted for 12–14.5 h. For the IPGTT, a dose of 2 g of glucose/kg body weight in a total volume of 200 μl saline solution was injected ip. For the insulin tolerance test (ITT), fed mice were separated 2 h before the experiment, and 1 IU/kg body weight of human insulin (Lilly; Humulina Regular) was injected ip in 200 μl total saline solution. For glucose sensitivity, we measured the incremental area under the curve (AUC) (23, 24).

To measure plasma insulin, mice were anesthetized with 70 mg/kg body weight sodium pentobarbital. Blood was obtained by cardiac puncture with a syringe containing EDTA. Levels of plasma insulin were determined by ELISA using the ultrasensitive mouse insulin assay kit from Mercodia AB (Uppsala, Sweden). In some samples from the fasted state experiment, insulin concentrations were below the detection level of the ELISA. These samples were three per condition and were given the value of the detection limit of the assay (0.025 μg/liter).

Western blot analyses

Freshly isolated islets were obtained by centrifugation and resuspended in cell lysis buffer (Cell Signaling Technology, Danvers, MA). Cell extracts were subjected to SDS-PAGE (12% gels). Prestained SDS-PAGE standards were included for molecular mass estimation. The transfer to polyvinylidene membranes was performed at 125 mA for 90 min in a buffer with 2.5 mM Tris base, 9 mM glycine, and 20% methanol. Membranes were blocked with 2% nonfat dry milk and incubated with the anti-sulfonylurea receptor 1 (Sur1) (1:100), anti-inward rectifier potassium channel 6.2 (Kir6.2) (1:500), and antiactin antibodies before being incubated with a peroxidase-conjugated donkey antigoat (Santa Cruz Biotechnology, Inc.) or goat antirabbit (GE Healthcare, Barcelona, Spain) antibodies, respectively. Protein bands were revealed by using the Enhanced Chemiluminiscence Reagents kit (Amersham Biosciences, Barcelona, Spain).

Reduced nicotinamide adenine dinucleotide (NADH) fluorescence

NADH autofluorescence was monitored using the same imaging system described for intracellular Ca^{2+} recordings. NADH fluorescence was excited with a 365-nm bandpass filter, whereas emission was filtered at 445 ± 25 nm (25). An image was acquired every 60 sec.

See Supplemental Materials and Methods published on The Endocrine Society's Journals Online web site at http://endo.endojournals.org.

Statistical analysis

Data are expressed as mean ± SE. Pairwise comparisons were made using Student's *t* test, unless otherwise stated. A probability level of 0.05 or lower was considered statistically significant.

Results

Activation of GC-A receptor by ANP increases insulin secretion and insulin content in intact islets of Langerhans

As described previously (12, 13), the ANP receptor, GC-A, is expressed in pancreatic cells, both β-cells and non-β-cells (Supplemental Fig. 1). 1 nM ANP increases insulin secretion in pancreatic islets stimulated with glucose as shown in Fig. 1A. This insulinotropic effect is not produced at lower ANP concentrations. The involvement of GC-A in this effect of ANP was studied on mice lacking GC-A. The insulin secretion in response to 7 mM glucose was similar in islets from GC-A WT and KO mice. The insulinotropic effect of ANP was fully inhibited in GC-A KO mice (Fig. 1B). In addition, 1 nM ANP also increased insulin content in islets of Langerhans within 1 h (Fig. 1C). This effect was only partially inhibited by the absence of GC-A.

ANP regulates K_{ATP} channel activity and glucose-induced $[Ca^{2+}]_i$ signals

We then studied the effect of ANP on K_{ATP} activity and observed that 1 nM ANP produced a decrease in K_{ATP} channel activity in WT β-cells (Fig. 2, A and B). This decreased activity evoked an increase in $[Ca^{2+}]_i$ in the presence of stimulatory glucose concentration, as shown in Fig. 2C. When the total entry of calcium into the cytosol was measured as the AUC/min, it was higher in the presence of ANP (Supplemental Fig. 2A). The potentiation of glucose-induced calcium signals is produced in islets obtained from different mouse strains and independently of sex (Supplemental Fig. 2B).

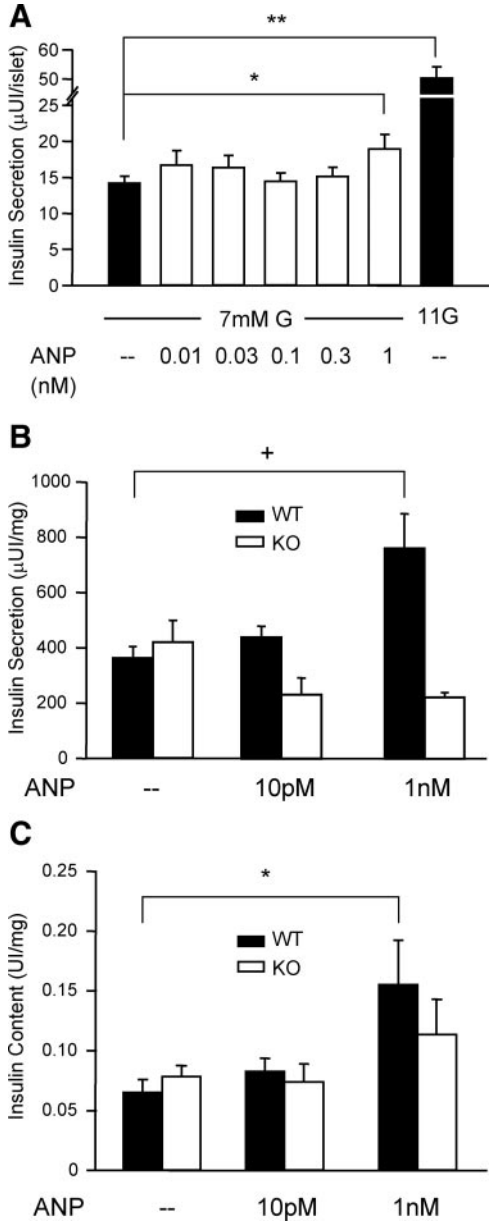

FIG. 1. ANP enhances insulin secretion and content in islets of Langerhans. A, Insulin secretion measurements at different ANP concentrations in 7 mM glucose (G); 11 mM glucose was used as internal control (n ≥ 70 islets/condition from 14 mice). B, Insulin secretion in response to 7 mM glucose plus 10 pM or 1 nM ANP in islets from WT (n ≥ 70 islets/condition, six mice) and GC-A KO mice (n ≥ 40 islets/condition, four mice). C, Insulin content measured in the islets after the secretion experiment in B. *, $P < 0.05$ *vs.* 7 mM glucose; +, $P < 0.01$ *vs.* 7 mM glucose; **, $P < 10^{-9}$ *vs.* 7 mM glucose.

Glucose regulation of insulin secretion in islets from GC-A KO mice

We sought to functionally characterize pancreatic β-cells in islets from GC-A KO mice. GSIS was enhanced in islets lacking GC-A. This effect was observed at both 11 and 16 mM glucose, whereas no genotype-dependent difference was observed under basal conditions or in response to 7 mM glucose (Fig. 3).

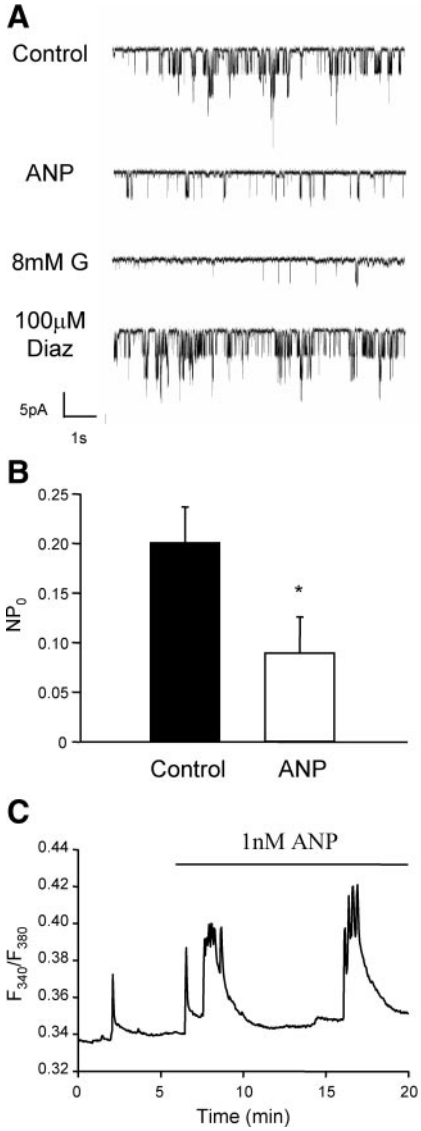

FIG. 2. ANP decreases the K_{ATP} channel activity and increases $[Ca^{2+}]_i$. A, A cell-attached patch-clamp recording of an isolated β-cell is shown. Several seconds of the same recording are shown at different moments of the experiment. Diaz, Diazoxide; G, glucose. B, The NP_o of the K_{ATP} channel during control and ANP treatment was measured (n = 3 cells). *, $P < 0.05$. C, $[Ca^{2+}]_i$ recording of an islet of Langerhans in the presence of 8 mM glucose; 1 nM ANP was added to the perfusion when indicated (n = 6 islets).

Islet size and insulin content in islets from GC-A KO mice

Islet size was measured as the islet area, and it was found that islets from GC-A KO were 13% smaller than those from WT mice (Fig. 4A). Moreover, when β-cell mass was measured, it tended to be lower at 2 months in GC-A KO mice ($P = 0.09$), and it was reduced at 8 months compared with WT ($P = 0.059$) (Fig. 4B). Notably, total pancreas weight was similar in WT and KO mice at both ages (Supplemental Fig. 3A). In addition, islets from GC-A KO mice presented a striking decrease in insulin content (Fig. 4C).

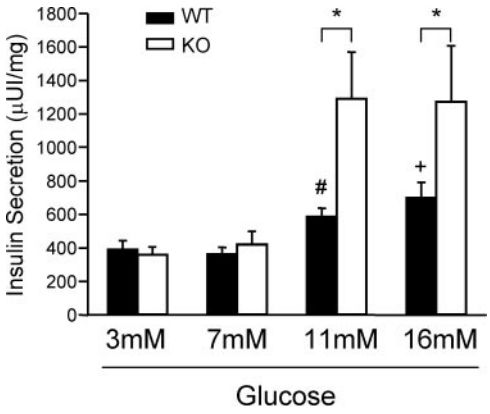

FIG. 3. Islets from GC-A KO mice secrete more insulin in response to glucose. Insulin secretion in response to increasing glucose concentrations in islets from WT (n ≥ 70 islets/condition, six mice) and GC-A KO mice (n ≥ 40 islets/condition, four mice). *, $P < 0.05$ *vs.* WT; #, $P < 0.05$ *vs.* 3 mM glucose; +, $P < 0.01$ *vs.* 3 mM glucose.

K_{ATP} channel activity and glucose-induced $[Ca^{2+}]_i$ signals in GC-A KO mice

The activity of the K_{ATP} was clearly diminished in β-cells from GC-A KO mice compared with WT in the absence of glucose (control; Fig. 5, A–C). The use of 100 μM diazoxide, a K_{ATP} channel opener, rendered decreased activity in GC-A KO β-cells compared with WT (Fig. 5, A–C). The channels in GC-A KO β-cells were, nonetheless, functional and responded to 8 mM glucose similarly to those from WT mice (Fig. 5, A, B, and D). The difference in the open probability of K_{ATP} with diazoxide suggested a decreased number of K_{ATP} channels in β-cells. Indeed, Western blot analyses demonstrated that both subunits of the channel, Sur1 and Kir6.2, were decreased in islets from GC-A KO mice when normalized to the levels of actin as the loading control (Fig. 6, A and B).

We then studied mitochondrial metabolism by measuring NADH concentration. There was no change at 3 mM glucose, a small increase in the response to 8 mM glucose, and no change was obtained at 16 mM glucose (Fig. 7, A and B). However, we observed that Ca^{2+} entry in response to 11 and 16 mM glucose was increased in islets from GC-A KO mice (Fig. 7C). This was measured as the percentage of time that the $[Ca^{2+}]_i$ remained elevated above 50% of the maximum level (Fig. 7D). Basal levels of intracellular calcium, at 3 mM glucose, did not differ between GC-A KO and WT mice (Supplemental Fig. 3B).

Glucose homeostasis in GC-A KO mice

We then analyzed blood glucose homeostasis in GC-A KO mice. For this purpose, IPGTT and ITT were performed. GC-A KO mice presented decreased body weight both at 3 and at 8 months (Supplemental Fig. 3D). However, they did not present either glucose intolerance or insulin resistance at any age tested (Fig. 8, A–C). In fact, when incremental AUC was measured for the IPGTT, it was significantly lower in GC-A KO mice at 8 months (Supplemental Fig. 3C).

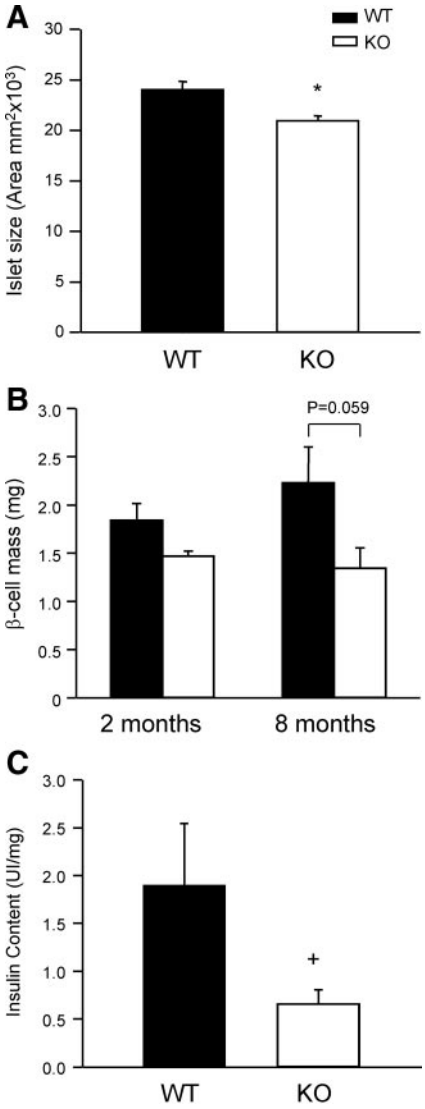

FIG. 4. Islets from GC-A KO mice present smaller size, lower β-cell mass, and lower insulin content. A, The islet size from GC-A WT and KO mice was calculated as the area at the widest diameter of the islet (n ≥ 400 islets/condition, three mice). B, β-Cell mass was measured in islets from WT and KO mice of 2 and 8 months old (n = 5–7 pancreas/condition). C, Insulin content from freshly isolated islets from GC-A WT and KO mice (n = 80–100 islets/condition, four to five mice). *, $P < 0.01$; +, $P < 0.05$.

When glycemia was measured in both fasted and fed states, the GC-A KO mice presented 20–30% increase in the fasted state at all ages (Fig. 8D). However, glycemia in the fed state was only statistically increased at 10 months old (Fig. 8E). When insulin plasma levels were measured, neither in the fasted nor in the fed states were they modified in GC-A WT *vs.* KO mice (Fig. 8F).

Discussion

In this work, we present evidence of an insulinotropic effect of ANP via activation of GC-A. This is reinforced by

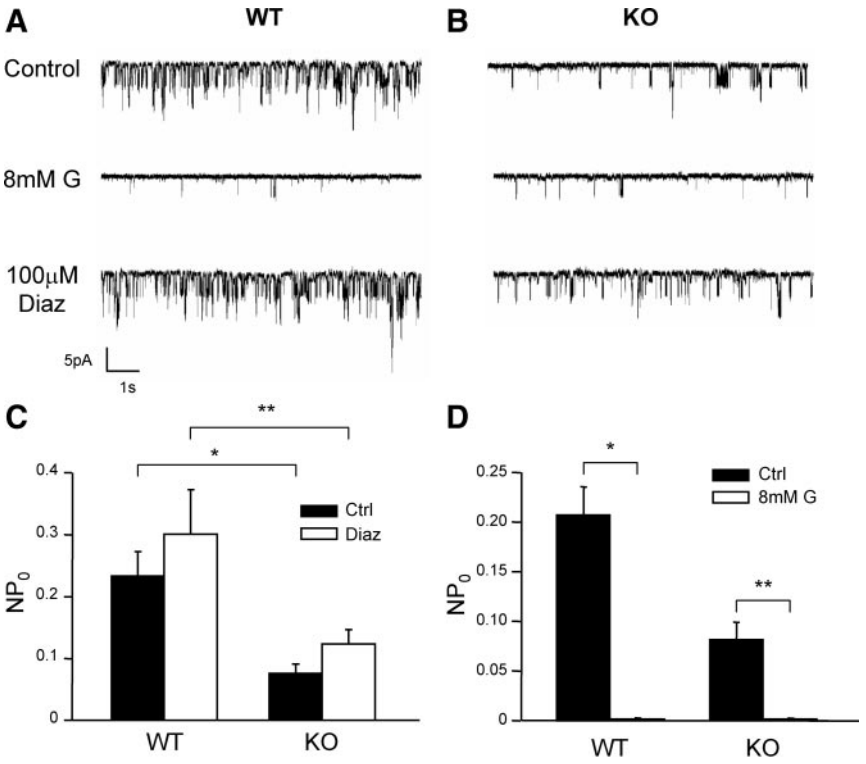

FIG. 5. K_{ATP} channel activity is diminished in GC-A KO mice. A, A cell-attached patch-clamp recording of an isolated β-cell from GC-A WT mice in the absence of glucose (G) [control (Ctrl)] and at different moments of the experiment. B, The same as in A but from a GC-A KO β-cell. C, Graph plotting NP_o in β-cells from GC-A WT and KO mice in control and 100 μM diazoxide (Diaz) (n = 6–7 cells per condition). *, $P < 0.01$ *vs.* WT; **, $P = 0.05$ *vs.* WT. D, NP_o in β-cells from GC-A WT and KO mice in control and 8 mM glucose (n = 4–5 cells/condition). *, $P < 0.0005$; **, $P < 0.005$ *vs.* control.

the ANP-induced reduction of K_{ATP} channel activity and the subsequent increase in $[Ca^{2+}]_i$. In addition, insulin content is also rapidly increased by ANP. The effect of ANP on β-cell function was abolished in islets from GC-A KO mice, indicating that it was dependent on GC-A. Islets from GC-A KO mice showed enhanced insulin secretion in response to increasing glucose concentrations, whereas basal insulin secretion did not change. This result was not the consequence of increased islet size or β-cell mass, because both were decreased in GC-A KO mice, as well as islet insulin content. Remarkably, basal K_{ATP} channel activity in GC-A KO β-cells was diminished as a result of the lowered Kir6.2 and Sur1 protein levels observed. In addition, the $[Ca^{2+}]_i$ response to increasing glucose concentrations was enhanced in GC-A KO mice. However, no change in mitochondrial metabolism was observed in GC-A KO mice that may explain the increase in GSIS. These mice were smaller and had normal IPGTT and ITT. GC-A KO mice presented, however, higher fasting glucose levels, although under 100 mg/dl.

Natriuretic peptides ANP and BNP are being involved in energy metabolism through the control of lipolysis in the adipose tissue (3). Recently, the overexpression of BNP in liver has been shown to protect against high-fat diet-induced increase in body weight and total fat weight. In addition, these mice presented increased fat oxidation. Insulin resistance, frequently associated with obesity, was also improved (4). A model has been proposed, in which ANP and BNP may be important in preventing obesity and type 2 diabetes (5). In contrast, the studies of the effect of ANP on insulin secretion have yielded discordant data. ANP has been shown to increase plasma insulin in humans (14) and GSIS in isolated rat islets (15). However, in other studies with rats, insulin secretion *ex vivo* did not change in response to ANP (17) or was even decreased after iv injection of the peptide (16). Our data show that ANP increases insulin secretion in mice islets in a GC-A-dependent manner. In addition, ANP blocks K_{ATP} channels and enhances Ca^{2+} signals in β-cells. This modulation of K_{ATP} and Ca^{2+} signals by ANP mimics the effects of cyclic GMP, the second messenger produced by the activation of GC-A by ANP, previously described in β-cells (18).

In the present work, we have used a wide range of ANP concentrations (10 pM to 1 nM). The effect of ANP on insulin secretion was only observed at 1 nM. In a series of studies in humans, ANP plasma concentration ranged within 250–800 pM in normal and obese patients (26, 27). However, other studies reported normal levels of ANP in the range of 1.1–13.7 pM for humans. Previous work reported basal levels of ANP of 159 ± 111 pM (n = 4) in GC-A WT and 279 ± 109 pM (n = 5) in GC-A KO mice (28). The higher circulating ANP concentration in GC-A KO mice is probably related to arterial hypertension and cardiac pressure overload and hypertrophy. Most of the physiological effects of ANP are through GC-A. However, we cannot rule out the possible involvement of NPR-C, the clearance receptor, because it has been shown to modulate the cAMP/AC and PLC signaling pathways (29, 30). Despite the discrepancy in normal plasma ANP levels, patients with heart or renal failure present higher ANP concentration (for review, please see Ref. 2). Therefore, the insulinotropic effect of ANP at high concentration may be important in regulating insulin secretion in heart and renal failure. In addition, it was suggested years ago by Atlas and Maack (31) that ANP can be produced locally at high concentrations acting as an emergency hormone to counteract stress situations by favoring vasodilation, natriuresis, and diuresis and maybe also insulin release if the target

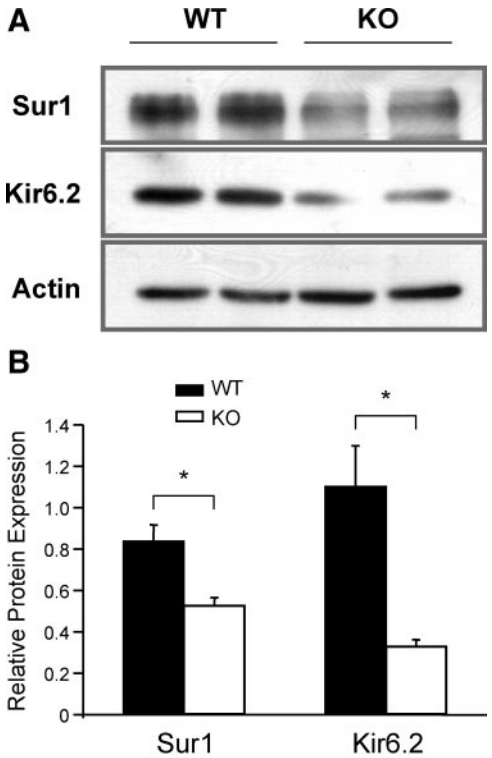

FIG. 6. K_{ATP} channel subunits expression is diminished in GC-A KO mice. A, Sur1 and Kir6.2 subunits of the K_{ATP} channel were analyzed by Western blotting. Actin is shown as loading control. B, Relative amount of Sur1 and Kir6.2 in islets from GC-A WT and KO mice with respect to actin (n = 3 mice/condition). *, $P < 0.05$ *vs.* WT.

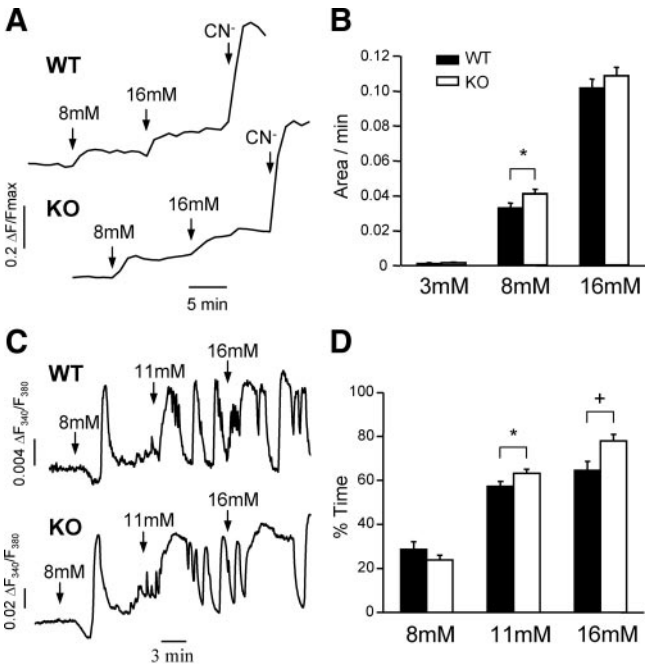

FIG. 7. Glucose-induced β-cell response is enhanced in GC-A KO mice. A, Two $[NADH]_i$ recordings of a GC-A WT (*upper panel*) and KO (*lower panel*) islet in response to glucose and cyanide (CN^-). Recordings start with 3 mM glucose. B, Graph plotting the AUC/min in response to different glucose concentrations (n = 13–14 islets/condition, two mice). *, $P = 0.05$. C, Two $[Ca^{2+}]_i$ recordings of a GC-A WT (*upper panel*) and KO (*lower panel*) islet in response to increasing glucose concentrations. D, Graph plotting the percentage of the time that calcium is elevated above half way at each glucose concentration from GC-A WT and KO mice (n = 16–17 islets/condition, three mice). *, $P < 0.05$; +, $P < 0.01$.

is the β-cell. In fact, recent studies suggested that ANP is produced within the pancreas itself (32). Other studies indicate that ANP is produced and released within the gastrointestinal mucosa, similarly as to incretin hormones (33). Hence, much higher local concentrations of ANP might occur in or around the pancreas.

Surprisingly, islets from GC-A KO mice responded to glucose with higher insulin secretion than WT islets, despite the smaller size and lower β-cell mass of GC-A KO mice. The decrease in β-cell mass may have a body weight-dependent component, because these two parameters are positively correlated (21). However, we cannot rule out an intrinsic defect in the regulation of β-cell mass in GC-A KO mice that showed increased body weight between months 2 and 8 without a concomitant increment in β-cell mass. In addition, You and Laychock (13) have recently shown that ANP, likely through GC-A activation, increases β-cell growth and [^{3}H] thymidine incorporation in rat islet DNA, via Akt phosphorylation. Therefore, it is plausible that in the absence of GC-A, islets of Langerhans compensated the reduced β-cell mass by enhancing GSIS. This adaptation may be produced by a decrease in the expression of the K_{ATP} subunits Sur1 and Kir6.2 and therefore by reducing K_{ATP} channel activity at basal levels, as described in the present work. K_{ATP} channels control the resting membrane potential and determine the electrical resistance of β-cells. When K_{ATP} channels are open and the membrane resistance is low, small currents will affect the plasma membrane potential (and therefore, insulin release) only minimally. However, when K_{ATP} channels are largely closed and membrane resistance is high, small currents will elicit the depolarization of the membrane, electrical activity, Ca^{2+} signals, and insulin release. Some of the features we encountered in these GC-A KO mice resemble some models described where the expression/function of K_{ATP} is lower or null (34–36). The increased GSIS (37, 38) and decreased islet size and β-cell mass (39) are shared with these models. However, some defects in blood glucose homeostasis and β-cell function described in these mice models, such as impaired GTT (39–41), were not present in GC-A KO mice. Therefore, the increase in GSIS observed in islets lacking GC-A may be the consequence of decreased K_{ATP} channel activity and subunit levels. However, we cannot explain the *in vivo* phenotype of the GC-A KO mice solely by the decrease of K_{ATP} channel activity. In addition, ANP is a pleiotropic hormone, and apart from its hypotensive and hypovolemic actions and role in blood pressure homeostasis, it has many different neuroendocrine and metabolic effects. In this model of global GC-A deletion, all cardiovascular and metabolic actions of ANP are ablated, and therefore, fine physiological experi-

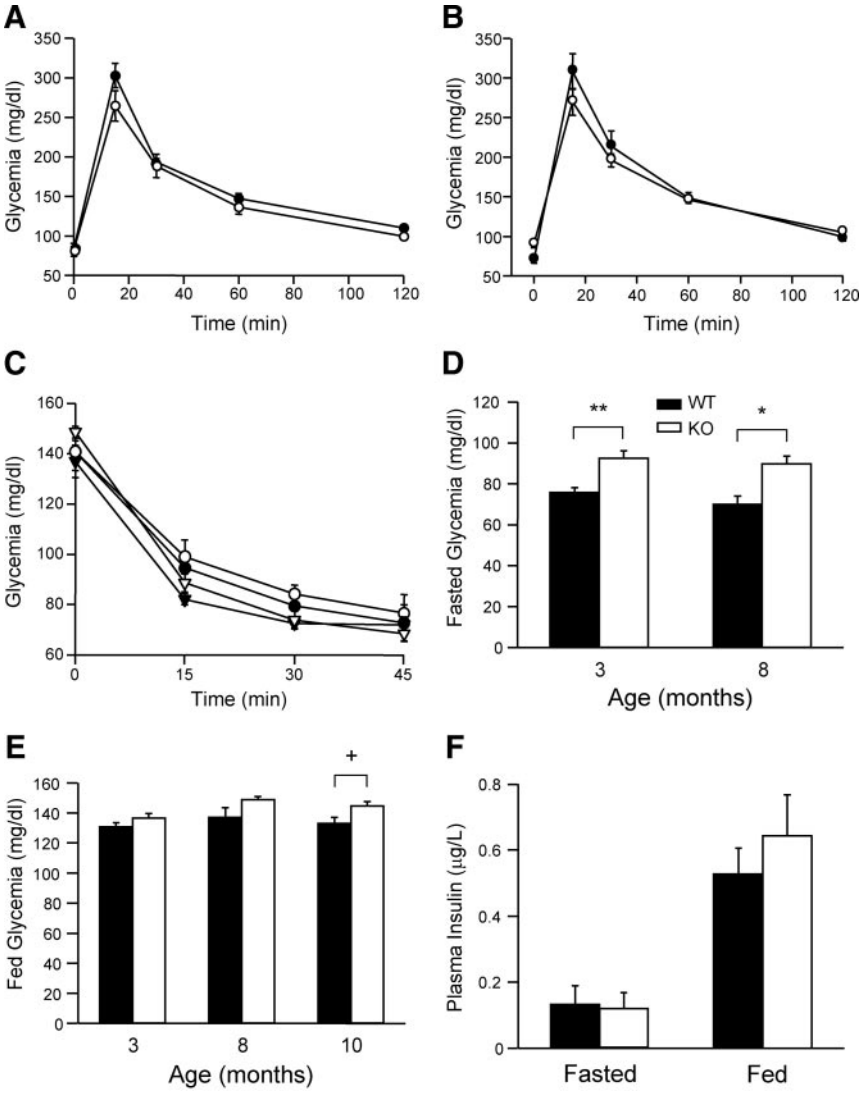

FIG. 8. Glucose and insulin sensitivities are not disrupted in GC-A KO mice. A, IPGTT was performed in 12-h-fasted 4-month-old GC-A WT and KO mice (n = 5 mice/condition). B, IPGTT was performed in 14.5-h fasted 8-month-old GC-A WT and KO mice (n = 6–7 mice/condition). C, ITT was performed in fed 4-month-old (n = 5 mice/condition) and 8-month-old (n = 7 mice/condition) GC-A WT and KO mice. ●, WT (4 months old); ○, KO (4 months old); ▼, WT (8 months old); ▽, KO (8 months old). D, Blood glucose concentration in GC-A WT and KO mice after 14.5 h of fasting at 3 (n = 11 mice per condition) and 8 months of age (n = 7 mice/condition). *, $P < 0.005$; **, $P < 0.001$. E, Blood glucose concentration in GC-A WT and KO mice in fed state in the morning at 3 (n = 10–11 mice per condition), 8 (n = 7 mice/condition), and 10 months of age (n = 6–7 mice/condition). +, $P < 0.05$. F, Plasma insulin concentration in 14.5-h fasted 4-month-old (n = 3 mice/condition) or fed 10-month-old GC-A WT and KO mice (n = 6–7 mice/condition).

ments are difficult to exert. Even more, subtle changes (for instance in glucose tolerance) might be masked by the complex phenotype observed in these mice (hypervolemic hypertension, cardiac hypertrophy).

Despite reduced islet size and β-cell mass, GC-A KO mice have normal glucose and insulin tolerance. It is plausible that the adaptation process by enhancing GSIS prevents the deterioration in glucose and insulin sensitivity. In fact, both defects in β-cell mass and β-cell function are required to develop diabetes, so that when one compensates the other, glucose tolerance is maintained unaltered (11). However, islets from GC-A KO mice may fail to properly respond to physiological situations in which insulin demand is increased and blood glucose homeostasis may be disrupted. In fact, GC-A −/+ mice fed with high-fat diet developed glucose intolerance, whereas the overexpression of BNP protected mice from developing high-fat diet-dependent insulin resistance (4).

The persistently higher fasting glucose levels in GC-A KO mice may be a consequence of liver defects. Fasting glycemia is mainly maintained by the hepatic endogenous glucose production (42), and in fact, hepatic insulin resistance is thought to be largely responsible for the development of fasting hyperglycemia (43).

The importance of regulating the expression of K_{ATP} subunits is not confined to β-cells. The K_{ATP} channel is also present in hypothalamic proopiomelanocortin neurons, and it is involved in insulin signaling, responsible for decreasing hepatic glucose production (44–47). In addition, K_{ATP} is also present in cardiomyocytes, where it plays a role in protecting the heart against cardiac stress (48). In fact, GC-A KO mice have a shorter life span and some of them suffer sudden death (49). The role that K_{ATP} may be playing in this event is not known.

In summary, there is increasing evidence supporting a role for natriuretic peptides and their receptors in metabolism and energy homeostasis (5). In this work, we present evidence indicating a direct effect of the ANP/GC-A signaling in β-cell function and suggesting that the endocrine pancreas should be considered an important target for natriuretic peptides and therefore contribute to their emerging role in metabolism.

Acknowledgments

We thank Ms. M. Luisa Navarro, Ana B. Rufete, and Jessica Escoriza for their excellent technical assistance and Dr. A. Rafacho for his help with statistics.

Address all correspondence and requests for reprints to: Ana B. Ropero, Institute of Bioengineering, Miguel Hernández University, 03202 Elche, Spain. E-mail: ropero@umh.es; or Angel Nadal, Institute of Bioengineering, Miguel Hernández University, 03202 Elche, Spain. E-mail: nadal@umh.es.

Present address for E.T.: Laboratory of Molecular and Cellular Medicine, Life Sciences Institute, University of British Columbia, Vancouver, Canada V6T 1Z3.

This work was supported by Ministerio de Ciencia e Innovación Grants BFU2008-01492 and BFU2007-67607, by the Generalitat Valenciana Grants GV/2009/056 and ACOMP/2010/113, by a Universidad Miguel Hernández-Bancaja grant, and by Fondo de Investigaciones Sanitarias 06/0891 from Instituto de Salud Carlos III. Centro de Investigación Biomédica en Red de Diabetes y Enfermedades Metabólicas Asociadas is an initiative of Instituto de Salud Carlos III. M.K. is supported by Sonderforschungsbereich 487.

Disclosure Summary: The authors have nothing to disclose.

References

1. **Kuhn M** 2003 Structure, regulation, and function of mammalian membrane guanylyl cyclase receptors, with a focus on guanylyl cyclase-A. Circ Res 93:700–709
2. **Potter LR, Abbey-Hosch S, Dickey DM** 2006 Natriuretic peptides, their receptors, and cyclic guanosine monophosphate-dependent signaling functions. Endocr Rev 27:47–72
3. **Lafontan M, Moro C, Berlan M, Crampes F, Sengenes C, Galitzky J** 2008 Control of lipolysis by natriuretic peptides and cyclic GMP. Trends Endocrinol Metab 19:130–137
4. **Miyashita K, Itoh H, Tsujimoto H, Tamura N, Fukunaga Y, Sone M, Yamahara K, Taura D, Inuzuka M, Sonoyama T, Nakao K** 2009 Natriuretic peptides/cGMP/cGMP-dependent protein kinase cascades promote muscle mitochondrial biogenesis and prevent obesity. Diabetes 58:2880–2892
5. **Moro C, Smith SR** 2009 Natriuretic peptides: new players in energy homeostasis. Diabetes 58:2726–2728
6. **Sarzani R, Salvi F, Dessì-Fulgheri P, Rappelli A** 2008 Renin-angiotensin system, natriuretic peptides, obesity, metabolic syndrome, and hypertension: an integrated view in humans. J Hypertens 26:831–843
7. **McKenna K, Smith D, Tormey W, Thompson CJ** 2000 Acute hyperglycaemia causes elevation in plasma atrial natriuretic peptide concentrations in Type 1 diabetes mellitus. Diabet Med 17:512–517
8. **Matsubara H, Mori Y, Yamamoto J, Inada M** 1990 Diabetes-induced alterations in atrial natriuretic peptide gene expression in Wistar-Kyoto and spontaneously hypertensive rats. Circ Res 67:803–813
9. **Nadal A, Alonso-Magdalena P, Soriano S, Ropero AB, Quesada I** 2009 The role of estrogens in the adaptation of islets to insulin resistance. J Physiol 587:5031–5037
10. **Kahn SE, Zraika S, Utzschneider KM, Hull RL** 2009 The β cell lesion in type 2 diabetes: there has to be a primary functional abnormality. Diabetologia 52:1003–1012
11. **Soria B, Quesada I, Ropero AB, Pertusa JA, Martin F, Nadal A** 2004 Novel players in pancreatic islet signaling: from membrane receptors to nuclear channels. Diabetes 53(Suppl 1):S86–S91
12. **Soriano S, Ropero AB, Alonso-Magdalena P, Ripoll C, Quesada I, Gassner B, Kuhn M, Gustafsson JA, Nadal A** 2009 Rapid regulation of K(ATP) channel activity by 17β-estradiol in pancreatic β-cells involves the estrogen receptor β and the atrial natriuretic peptide receptor. Mol Endocrinol 23:1973–1982
13. **You H, Laychock SG** 2009 Atrial natriuretic peptide promotes pancreatic islet β-cell growth and Akt/Foxo1a/cyclin D2 signaling. Endocrinology 150:5455–5465
14. **Uehlinger DE, Weidmann P, Gnädinger MP, Hasler L, Bachmann C, Shaw S, Hellmüller B, Lang RE** 1986 Increase in circulating insulin induced by atrial natriuretic peptide in normal humans. J Cardiovasc Pharmacol 8:1122–1129
15. **Fehmann HC, Noll B, Goke R, Goke B, Trautmann ME, Arnold R** 1990 Atrial natriuretic factor has a weak insulinotropic action in the isolated perfused rat pancreas. Res Exp Med 190:253–258
16. **Ahrén B** 1988 ANF inhibits glucose-stimulated insulin secretion in mouse and rat. Am J Physiol 255:E579–E582
17. **Verspohl EJ, Ammon HP** 1989 Atrial natriuretic peptide (ANP) acts via specific binding sites on cGMP system of rat pancreatic islets without affecting insulin release. Naunyn Schmiedebergs Arch Pharmacol 339:348–353
18. **Ropero AB, Fuentes E, Rovira JM, Ripoll C, Soria B, Nadal A** 1999 Non-genomic actions of 17 β-estradiol in mouse pancreatic β-cells are mediated by a cGMP-dependent protein kinase. J Physiol 521:397–407
19. **Lopez MJ, Wong SK, Kishimoto I, Dubois S, Mach V, Friesen J, Garbers DL, Beuve A** 1995 Salt-resistant hypertension in mice lacking the guanylyl cyclase-A receptor for atrial natriuretic peptide. Nature 378:65–68
20. **Nadal A, Rovira JM, Laribi O, Leon-quinto T, Andreu E, Ripoll C, Soria B** 1998 Rapid insulinotropic effect of 17β-estradiol via a plasma membrane receptor. FASEB J 12:1341–1348
21. **Montanya E, Nacher V, Biarnés M, Soler J** 2000 Linear correlation between β-cell mass and body weight throughout the lifespan in Lewis rats: role of β-cell hyperplasia and hypertrophy. Diabetes 49:1341–1346
22. **Montanya E, Téllez N** 2009 Pancreatic remodeling: β-cell apoptosis, proliferation and neogenesis, and the measurement of β-cell mass and of individual β-cell size. Methods Mol Biol 560:137–158
23. **Abdul-Ghani MA, Matsuda M, Balas B, DeFronzo RA** 2007 Muscle and liver insulin resistance indexes derived from the oral glucose tolerance test. Diabetes Care 30:89–94
24. **Cooksey RC, Jouihan HA, Ajioka RS, Hazel MW, Jones DL, Kushner JP, McClain DA** 2004 Oxidative stress, β-cell apoptosis, and decreased insulin secretory capacity in mouse models of hemochromatosis. Endocrinology 145:5305–5312
25. **Quesada I, Todorova MG, Soria B** 2006 Different metabolic responses in α-, β-, and δ-cells of the islet of Langerhans monitored by redox confocal microscopy. Biophys J 90:2641–2650
26. **Wang TJ, Larson MG, Levy D, Benjamin EJ, Leip EP, Wilson PW, Vasan RS** 2004 Impact of obesity on plasma natriuretic peptide levels. Circulation 109:594–600
27. **McMurray Jr RW, Vesely DL** 1992 Weight reduction decreases the circulating concentration of the N terminus of the ANF prohormone. Am J Med Sci 303:2–8
28. **Lopez MJ, Garbers DL, Kuhn M** 1997 The guanylyl cyclase-deficient mouse defines differential pathways of natriuretic peptide signaling. J Biol Chem 272:23064–23068
29. **Anand-Srivastava MB** 2005 Natriuretic peptide receptor-C signaling and regulation. Peptides 26:1044–1059
30. **Rose RA, Giles WR** 2008 Natriuretic peptide C receptor signaling in the heart and vasculature. J Physiol 586:353–366
31. **Atlas SA, Maack T** 1987 Effects of atrial natriuretic factor on the kidney and the renin-angiotensin-aldosterone system. Endocrinol Metab Clin North Am 16:107–143
32. **Valentino B, Lipari D, Peri G, Lipari L, Valentino A, Farina E** 2009 ANP and insuin presence in human fetal pancreas. Ital J Anat Embryol 114:21–25
33. **Qiu ZX, Mei B, Wu YS, Huang X, Wang ZY, Han YF, Lu HL, Kim TC, Xu WX** 2010 Atrial natriuretic peptide signal pathways up-regulated in stomach of streptozotocin-induced diabetic mice. World J Gastroenterol 16:48–55
34. **Seino S, Miki T** 2004 Gene targeting approach to clarification of ion channel function: studies of Kir6.x null mice. J Physiol 554:295–300

35. **Minami K, Miki T, Kadowaki T, Seino S** 2004 Roles of ATP-sensitive K+ channels as metabolic sensors: studies of Kir6.x null mice. Diabetes 53(Suppl 3):S176–S180
36. **Aittoniemi J, Fotinou C, Craig TJ, de Wet H, Proks P, Ashcroft FM** 2009 Review. SUR1: a unique ATP-binding cassette protein that functions as an ion channel regulator. Philos Trans R Soc Lond B Biol Sci 364:257–267
37. **Koster JC, Remedi MS, Flagg TP, Johnson JD, Markova KP, Marshall BA, Nichols CG** 2002 Hyperinsulinism induced by targeted suppression of β cell KATP channels. Proc Natl Acad Sci USA 99:16992–16997
38. **Remedi MS, Rocheleau JV, Tong A, Patton BL, McDaniel ML, Piston DW, Koster JC, Nichols CG** 2006 Hyperinsulinism in mice with heterozygous loss of K(ATP) channels. Diabetologia 49:2368–2378
39. **Miki T, Tashiro F, Iwanaga T, Nagashima K, Yoshitomi H, Aihara H, Nitta Y, Gonoi T, Inagaki N, Miyazaki J, Seino S** 1997 Abnormalities of pancreatic islets by targeted expression of a dominant-negative KATP channel. Proc Natl Acad Sci USA 94:11969–11973
40. **Miki T, Nagashima K, Tashiro F, Kotake K, Yoshitomi H, Tamamoto A, Gonoi T, Iwanaga T, Miyazaki J, Seino S** 1998 Defective insulin secretion and enhanced insulin action in KATP channel-deficient mice. Proc Natl Acad Sci USA 95:10402–10406
41. **Seghers V, Nakazaki M, DeMayo F, Aguilar-Bryan L, Bryan J** 2000 Sur1 knockout mice. A model for K(ATP) channel-independent regulation of insulin secretion. J Biol Chem 275:9270–9277
42. **Roden M, Bernroider E** 2003 Hepatic glucose metabolism in humans—its role in health and disease. Best Pract Res Clin Endocrinol Metab 17:365–383
43. **Biddinger SB, Kahn CR** 2006 From mice to men: insights into the insulin resistance syndromes. Annu Rev Physiol 68:123–158
44. **Obici S, Zhang BB, Karkanias G, Rossetti L** 2002 Hypothalamic insulin signaling is required for inhibition of glucose production. Nat Med 8:1376–1382
45. **Pocai A, Lam TK, Gutierrez-Juarez R, Obici S, Schwartz GJ, Bryan J, Aguilar-Bryan L, Rossetti L** 2005 Hypothalamic K(ATP) channels control hepatic glucose production. Nature 434:1026–1031
46. **Sandoval D, Cota D, Seeley RJ** 2008 The integrative role of CNS fuel-sensing mechanisms in energy balance and glucose regulation. Annu Rev Physiol 70:513–535
47. **Lam CK, Chari M, Lam TK** 2009 CNS regulation of glucose homeostasis. Physiology 24:159–170
48. **Burke MA, Mutharasan RK, Ardehali H** 2008 The sulfonylurea receptor, an atypical ATP-binding cassette protein, and its regulation of the KATP channel. Circ Res 102:164–176
49. **Oliver PM, Fox JE, Kim R, Rockman HA, Kim HS, Reddick RL, Pandey KN, Milgram SL, Smithies O, Maeda N** 1997 Hypertension, cardiac hypertrophy, and sudden death in mice lacking natriuretic peptide receptor A. Proc Natl Acad Sci USA 94:14730–14735